

Density Functional Theory Based Understanding on the Reactivity of N₂ Molecule on Al_n (n = 2, 3, 13, 30 and 100) Clusters

Bhakti S. Kulkarni[†], Sailaja Krishnamurthy^{*,‡} and Sourav Pal^{*,†}

[†]*Physical Chemistry Division, National Chemical Laboratory (CSIR), Pune 411008*

[‡]*Functional Materials Division, Electrochemical Research Institute (CECRI) (CSIR), Karaikudi 630 006*

Abstract

Reactivity of Aluminum Clusters has been found to exhibit size sensitive variations. This work is motivated by a recent report¹ predicting higher reactivity of melted Aluminum clusters towards the N₂ molecule as compared to the non-melted Al clusters. We attempt to understand the underlying electronic and structural factors influencing the adsorption of N₂ molecule (a prerequisite for the reactivity) on ground state geometry (a non-melted structure) of various Al clusters. The results show that the adsorption energy is of the order of 8-10 kcal/mol and does not vary with respect to the cluster size and the electronic properties of the ground state geometry. The structural and electronic properties of high energy conformations of Al clusters (a melted cluster) are also analyzed to explain their higher reactivity towards N₂ molecule.

***Corresponding author, E-mail: sailaja.raaj@gmail.com; s.pal@ncl.res.in**

I. Introduction

The appearance of the bulk motif in small sized aluminum clusters has excited many researchers. As a consequence of this property, Al clusters are attracting a lot of attention for their potential applications in optics, medicines,² microelectronics³ and nanocatalysis⁴. In addition to the appearance of bulk motif, ground state Al_n clusters ($n < 100$) show size specific features in their structures,⁵⁻⁸ cohesive energies,⁹⁻¹¹ and thermodynamic properties.¹²⁻¹⁴ For example, the ground state geometries of many clusters are seen to change from a disordered morphology to an ordered one (or vice-versa) with the addition of a single atom.¹⁵ Adding an extra atom to some clusters also changes the melting transition from a first-order to a second order.¹⁶⁻²² The above mentioned and many other size dependent characteristics make the study and application of aluminum nano clusters with up to a few hundred atoms both interesting and challenging.

One such application is the synthesis of aluminum nitride. Aluminum nitride, one of the industrially important materials, carries high impact as an electronic material and is usually synthesized through a direct reaction between Al surface or clusters and N_2 at a high temperature and pressure²³. Nevertheless, one needs to modify a processing condition to smoothen such tedious and hard reactions. Consequently, recent experimental studies showing that Al clusters of range 25-100 have melting temperatures that are 450 K, well below the bulk melting temperature, 934 K has excited the several researchers²². Not only clusters in this range show a depressed melting temperature, they also show a size sensitive melting behavior. These results can be exploited to design the chemical reactions at desired temperature by choosing an appropriate cluster. In addition, the depressed melting temperature of clusters facilitates easier chemisorption and thus various chemical reactions at very low temperatures (around 450 K). It is noteworthy that N_2 molecule is only known to physisorb on the Al surfaces below the melting temperatures²⁴ and thus use of clusters for such reactions could be more advantageous.

The above aspect is demonstrated very nicely in a recent report by Jarrold *and co-workers*¹ where they discuss the reactivity of N_2 on Al_{100} cluster. They have determined the melting temperature

of Al₁₀₀ using heat capacity measurements following which the ion beam experiments are used to investigate the reaction between the cluster and molecular N₂. They show that above the melting transition, the activation barrier for N₂ adsorption decreases nearly by 1 eV. The importance of Al-N reaction has also motivated Romanowski *et. al.*²⁵ to perform a theoretical study of N₂ reaction with liquid Al metal. They have determined the activation barrier for dissociative chemisorption of N₂ to be 3.0 eV. They propose that the melting decreases the surface energy, and atoms in liquid are mobile and better able to adjust the N₂ molecule. Hence, previous studies on N₂ adsorption conclude that the atoms on the surface of the liquid cluster move to minimize their energy lowering the activation barrier.

Apart from the enhanced mobility, very little understanding is available concerning the role of structure and bonding of Al clusters on the adsorption/reactivity of the cluster. The catalytic reactivity is always attributed to specific and precise structural rearrangement of atoms in the material. It is worthwhile to correlate the above two parameters to their reactivity. Thus, the interesting questions are: “Is the chemisorption of N₂ molecule a consequence of highly different structure of Al cluster following the phase transition? Do the changes in structure modify the chemical bonding property within the cluster thereby enhancing its reactivity or the higher reactivity is due the dynamical rearrangement of atoms within cluster? Does this reactivity vary as a function of cluster size?” To answer the above questions, we have studied systematically the adsorption behavior of N₂ on Al cluster as a function of cluster size. We also address the issue of conformational changes following the phase transition and their impact on N₂ adsorption.

To achieve this objective, we choose a series of Al clusters of variable size. It includes low energy conformers of Al₂, Al₃, Al₁₃, Al₃₀ and Al₁₀₀ clusters. Al₂ and Al₃ are the smallest of Al clusters that have been analyzed for understanding the adsorption of N₂ molecule. The reason for starting with such small clusters is to have a qualitative understanding on two issues viz., (a) to understand the electronic properties underlying the adsorption of the molecule on the cluster. (b) to analyze the adsorption of N₂ molecule as a function of Al cluster size. After analyzing the various reactive sites of

these clusters, N_2 is adsorbed on them to study its interactive nature. The zero-temperature studies of adsorption is extended to a decahedron conformer as well as a few high energy conformers of Al_{13} (typically seen after the phase transition) to analyze the ease of adsorption on high energy conformations. Since melting enhances distortion, these high energy structures help us to correlate the specific role of structure and bonding towards chemisorption of N_2 . All considered structures were optimized and the bonding properties within them are analyzed through Electron Localization Function (ELF) and Frontier Molecular Orbital (FMO).

The rest of the work is organized as follows. In Section II, we give a brief description of the computational method and descriptors of reactivity used in this work. Results and discussion are presented in section III for Al_n -- N_2 interaction. Finally, our conclusions are summarized in section IV.

II. Computational Details

As mentioned, we have considered aluminum clusters of varying sizes viz.,: Al_2 , Al_3 , Al_{13} , Al_{30} and Al_{100} for the study. All the possible conformations of these clusters are optimized. Following the optimization, low lying structures are considered for further study of adsorption. All the structures were optimized using Density Functional Theory (DFT) based method. The optimization is carried out using VASP.^{26, 27} As in standard DFT programs, the stationary ground state is calculated by solving iterative Kohn-Sham equations.²⁸ We use Vanderbilt's ultra-soft pseudo-potentials²⁹ within the Local Density Approximation (LDA) for describing the behavior of core electrons. An energy cut-off of 400 eV is used for the plane wave³⁰ expansion of Al and N atoms. The structural optimization of all geometries is carried out using the conjugate gradient method,³¹ except for the high energy conformers where, we use *quasi-Newton* method³² in order to retain the local minima. The structure is considered to be optimized when the maximum force on each atom is less than 0.01 eV/Å. Similar optimization procedures are repeated for the interaction of N_2 molecule at all Al cluster reactive sites, and for that of bare N_2 molecule. All the molecules are enclosed in cubical box of 25 Å dimensions.

Various descriptors are used to analyze the reactivity of the Al clusters. One such is Electron

Localization Function (ELF) modified and applied by Silvi and Savin.³³ According to this description, the molecular space is partitioned into regions or basins of localized electron pairs or attractors. At very low value of ELF all the basins are connected. As this value increases, the basins begin to split and finally, we will get as many basins as the number of atoms. Typically, the existence of an iso-surface in the bonding region between two atoms at a high value of ELF say >0.70, signifies localized bond in that region. The mathematical description of ELF is as follows,

$$\eta(r) = \frac{1}{1 + \left(\frac{D_p}{D_h}\right)^2} \quad (2.1)$$

$$D_h = \left(\frac{3}{10}\right)(3\pi^2)^{5/3} * \rho^{5/3} \quad (2.2)$$

$$D_p = \frac{\frac{1}{2} \sum_i |\nabla \psi|^2 - \frac{1}{8} |\nabla \rho|^2}{\rho} \quad (2.3)$$

$$\rho = \sum_{i=1}^N |\psi(r)|^2 \quad (2.4)$$

where the sum in Eqn. 2.4 is over all the occupied orbitals. D_h is the kinetic energy of the electron gas having the same density or one can say its the value of D_p in a homogeneous electron gas and ρ is the charge density.

We have analyzed the ELF for all clusters and their complexes of N_2 at isovalue where atomic basins start merging. Thus, as size and geometry of Al cluster changes, here, the ELF analysis helps us to understand the discrete bonding pattern. In addition, we also analyze the partial charge densities of FMO. The Highest Occupied Molecular Orbital (HOMO) and Lowest Unoccupied Molecular Orbital (LUMO) are the best used global descriptors of reactivity.^{34-36a} The N_2 adsorption at particular site is followed by HOMO and LUMO analysis, which helps to distinguish the most reactive site. Subsequently, after complex formation, same descriptors elaborate the peculiar Al-N bonding. In

addition, to understand the over all charge distribution after complex formation, the charges on various atoms (in optimized bare clusters and respective complexes) are calculated through the GAMESS^{36b} considering the single point energy convergence.

Following the studies on the ground state conformations of Al clusters of varying sizes, as mentioned, we have considered few high energy conformations of Al₁₃ for N₂ adsorption. This is done with an aim of elucidating the role of electronic properties of these high energy melted conformations on the chemisorption. One of the earlier theoretical works has reported that Al₁₃ undergoes a solid to liquid transition between 1000-1700 K³⁷. Hence, the high energy conformations are obtained from a finite temperature run of Al₁₃ at 1200 and 1600K. It may be recalled that an earlier work³⁷ predicted 1600K to be nearly melting temperature of the cluster. The finite temperature calculations are performed by using Born-Oppenheimer molecular dynamics based on the Kohn-Sham formulation of DFT, employed in VASP. The ionic phase space of the cluster is sampled classically in a canonical ensemble using a method proposed by N ose³⁸. Pursuing the simulation of 10 pico seconds, few conformations were chosen from these high temperature runs. The structure, bonding and reactivity of these clusters are discussed and compared with those of the low lying conformation of the same cluster.

III. Results and Discussion:

(a) Ground State Geometries of Al clusters and their Interaction with N₂:

(i) Structure, Bonding of Al₂ and its Interaction with N₂ molecule:

Al₂ like any mono atomic dimer cluster is a covalently bonded one,³⁹⁻⁴³ while Al₃ is a widely studied system for adsorption of various molecules such as H₂⁴⁴⁻⁴⁶, O₂⁴⁷ etc. Figure 1 gives the ground state geometries of Al₂ and their complexes with N₂. The ELF contours and the frontier orbitals for these systems are given in the same Figure. Various inter atomic distances along with the Mulliken charges on each atom [in square bracket] for Al₂ and Al₂--N₂ are given in the same Figure.

We begin with a discussion of Al₂ followed by its complex with N₂. The inter atomic bond distance in Al₂ is 2.59  . This is in perfect agreement with the reported literature values.³⁹⁻⁴³ The

covalent nature of Al_2 is well seen from the contours of ELF, where both Al basins merge considerably around a value of 0.76. The FMO analysis predicts that HOMO orbital is bonding orbital (σ -overlap) and LUMO is localized on the two Al atoms (p-orbitals). The favorable mode of N_2 interaction with Al_2 is a linear structure as seen from Figure 1. Other modes of interaction (perpendicular to the Al-Al bond of Al_2 molecule) do not result in local minima. The Al_2 -- N_2 complex has an interaction energy of -0.57 eV (-13.10 kcal/mol). Following the adsorption of N_2 molecule, the Al-Al and N-N bond distances increase marginally from 2.59 to 2.61 Å and from 1.11 to 1.15 Å, respectively. The Al_2 -- N_2 interaction optimizes at an Al-N distance of 1.86 Å. The corresponding ELF contours at an isovalue of 0.76 reveals a polarized electron density on Al(2) and N(1) atoms (see Figure 1). There are no merged basins in the Al-N bonding region even at an isovalue of 0.50.

The HOMO of Al_2 -- N_2 complex is composed of 2p orbitals of N atoms while the LUMO is composed of p orbitals of interacting Al atom and N_2 atoms. To understand the charge redistribution following the adsorption of N_2 , we study the difference charge density ($\Delta\rho$) (Figure 1). The blue region indicates charge gained where as the red region indicates the charge depletion. The presence of red region along the N_2 and Al_2 bonds and presence of blue region around the each atom shows a small polarization within the whole molecular space. Thus, Al_2 and N_2 , in their interaction show an overall charge transfer from Al_2 to N_2 . In order to quantify the charge transfer we have calculated the Mulliken charges for individual systems and the complex. The charges of Al atoms in the individual Al_2 are 6.6×10^{-4} a. u. and -6.6×10^{-4} a. u respectively (and hence nearly zero). The corresponding charges on Al atoms in the complex are 0.123 a. u. (non-interacting Al atom) and 0.513 a. u (interacting Al atom). The N(1) atom (interacting N atom) in N_2 shows charge gain of -1.202 a. u. while N(2) is slight positively charged. Thus, both the difference charge density and Mulliken charges reveal an over all charge transfer from Al_2 to the N_2 molecule.

The moderate interaction energy of N_2 with Al dimer promotes us to study the nature of N_2 interaction as a function of cluster size and geometry. Does the bonding remain same for larger cluster

sizes? Does interaction energy increase with the cluster size? Various such questions will be addressed in the next few sections.

(ii) Structure, Bonding of Al₃ and its Interaction with N₂ molecule:

A three atom cluster has three possible geometric configurations viz., linear conformation, zig-zag conformation and a cyclic conformation.^{48, 49} The three conformations in Al₃ differ from each other by nearly 1 eV with cyclic Al₃ as the most stable configuration. This is consistent with earlier literature reports.^{48, 49} Cyclic Al₃ is an equilateral triangle as shown in Figure 2 with Al-Al bond distances of 2.47 Å. Thus, we note a decrease in the inter atomic bond distance within the Al atoms as compared to the Al₂. In spite of the decreased bond distances, the ELF basins merge only at a value of 0.74 as compared to 0.76 in Al₂. The HOMO of Al₃ shows a multi centered bonding arising from the overlap of s-p hybridized orbitals. The LUMO is made up of p orbitals of Al atoms. Considering the orbital contributions and their density contours, we verified two modes for N₂ adsorption. One perpendicular to the plane of triangle and another along one of the Al-Al bonds as shown in Figure 2. The first Al₃--N₂ conformation was found to be a meta stable one with N₂ getting desorbed. However, the second Al₃--N₂ configuration resulted in a stable minima with an interaction energy of -0.47 eV (i. e. -10.77 kcal/mol). Interestingly this is nearly 3 kcal/mol lower than that of dimer complex.

N₂ adsorption reduces the symmetry of the Al₃ cluster from an equilateral triangle to an nearly isosceles triangle. The Al(2)-Al(3) (see Figure 2) increases to 2.64 from 2.47 Å with rest of the two Al-Al bond lengths remaining around their original values. The Al-N interaction converges to the same bond length as that in Al₂--N₂ complex i. e., 1.86 Å. The N₂ bond also increases to 1.15 Å from 1.11 Å like in the case of Al₂--N₂. The ELF contour of the complex (at an isovalue of 0.80) shows polarization of densities on Al(3) atom (the Al atom interacting with N₂) and N(1) atom. Similar to Al₂--N₂ complex, Al₃--N₂ complex does not show merged basins in the Al-N bonding region. The frontier orbital analysis shows that HOMO is contributed by the p orbitals of N₂, Al(3) and Al(2) atoms. The LUMO is composed of bonding orbital of Al(1) and Al(2) atoms (the two Al atoms not interacting with N₂). The

charges derived by Mulliken population analysis for Al_3 and $\text{Al}_3\text{--N}_2$ are given in Figure 2. All the atoms in the Al_3 are nearly neutral in the cluster as well as the complex. However, the N_2 molecule is polarized following the complexation. However, the difference charge density plot shown in Figure 2 reveals that there has been some charge redistribution among the Al and N atoms. Each atom is seen to donate some electrons from one of its orbital and gain in another of its atomic orbital there by neutralizing the overall charge transfer. Thus, Al_3 , shows a marginal decrease in the interaction energy.

(iii) Structure, Bonding of Al_{13} and its Interaction with N_2 molecule:

Our next cluster to be studied for N_2 adsorption is an Al_{13} cluster. Al_{13} is the most well studied among the aluminum clusters. Icosahedra (I_h) is indebted global minima in all extensive static and dynamic studies of Al_{13} .⁵⁰ Hence, we found it interesting to chose this as the next larger cluster for N_2 adsorption. Figure 3a shows optimized geometries of I_h , and its N_2 complex. We now classify atoms within the cluster in order to facilitate the discussion of various reactive sites with the cluster and the N_2 adsorption on them. The Various atomic sites in the I_h conformation can be classified into three types viz., “A”, “B” and “C” depending upon their chemical environment and their distances from the central atom (see Figure 3a). Site A is the single central atom. Site B and C are the surface atoms containing six atoms each. The atoms “B” lie at a distance of 2.66 Å from the central atom “A” and atoms “C” lie at a distance from 2.60 Å from central atom “A”. Figure 3b shows another perspective of the I_h conformation for a better understanding of the reactive sites. Thus, the structure is highly symmetric. Table 1 gives details of these inter atomic distances between various types of sites. Distances between two adjacent “B” atoms is 2.82 Å, while that of two adjacent “C” atoms is 2.90 Å. Owing to their different orientations with respect to the central atom “A”, the inter atomic distance between two diagonally placed “B” atoms is 5.32 Å while the distance between “C” atoms is 5.21 Å. The inter-atomic distance between site “B” and “C” is 2.70 Å.

This symmetry is reflected in Mulliken atomic charges (tabulated in Table 1) and ELF isosurfaces (seen in Figure 3a). The site A, is positively charged with 3.43 a. u., sites “B” and “C”

attracting a negative charge of -0.3 and -0.28 a. u., respectively. Analysis of ELF basins shows that ELF basins do not merge until a isovalue of 0.75. Around 0.74, basins corresponding to sites “B” and “C” merge with each other. Interestingly, basins of adjacent “B” do not merge with each other. Same is the case for adjacent “C” atoms. These basins merge at a slightly higher value of 0.72. These results indicate an overall covalent nature of the bonds (as in case of Al₂ and Al₃ clusters), with stronger sharing between the negatively charged “B” atoms with negatively charged “C” atoms. These bonding peculiarities of I_h geometry are also reproduced in the FMO’s. Analysis of HOMO reveals a multi centered bonding contributed by “C” atoms in the same plane as seen in Figure 3a. However, the LUMO is contributed by only “B” atoms.

Following the analysis of FMO and ELF, site “B” and “C” appear to be susceptible⁵¹ to the N₂ attack. Hence, we have studied the adsorption of N₂ on both these sites. The adsorption of N₂ on site “B” results in a meta-stable structure with finally N₂, desorbing from it. The adsorption of N₂ on site “C” results on the other hand in a stable conformation with an interaction energy of -0.34 eV (-7.91 kcal/mol). Interestingly, this is nearly half of that found for O₂ molecule on Al₁₃ (-0.77 eV) reported by Shiv Khanna and co-workers⁴⁷. They attribute such a low interaction energy of Al₁₃ to its magic cluster property (exceptional stability) and hence its nonreactive behavior towards many reagents. The marginally lower interaction energy of Al₁₃ towards N₂ molecule as compared to Al₂ and Al₃ is reflected in its Al-N bond distance (which is 1.90 Å as compared to 1.86 Å in Al₂ and Al₃ complex). The N-N bond distance in the complex is 1.13 Å as compared to 1.15 Å in Al₂ and Al₃.

Following the N₂ adsorption there is a small loss of symmetry. For the sake of better understanding of structural changes following the adsorption we rename the interacting “C” atom as “C_{int}”. The “A”-“C” bond distance in the Al₁₃(I_h)-N₂ complex reduces to 2.54 Å from 2.60 Å, “A”-“C_{int}” increases to 2.63 Å from 2.60 Å. Similarly, “B”-“C” bonds increase to 2.78 Å from 2.70 Å. The “A”-“B” and “B”-“B” bond distances in the complex remain around their original values. The distance between “C”-“C” is 2.86 Å in the complex as compared to “C”-“C” distance of 2.90 Å in I_h. The

interatomic distances between the diagonally opposite “B” atoms in complex is 5.50 Å (as compared to 5.32 Å) and that between diagonally opposite “C” atoms is 5.28 Å (as compared to 5.21 Å). Thus, the volume of the cluster increases marginally following the N₂ adsorption.

Analysis of FMO's shows that HOMO is contributed by the interacting Al atom, and some lower plane of atoms in the cluster. The charge distribution in Al₁₃--N₂ complex is given in Table 1. There is an overall charge transfer of 0.21 electrons to N₂ from Al₁₃ atom. It may be noted that this is less than that seen in Al₂ but more than what is seen for Al₃. The Al atom bonded to the N₂ molecule acquires a positive charge of 0.81 a. u. As a consequence, following the charge transfer (see Figure 3c), the atoms on upper half (atoms above the central atom “A”) of Al₁₃ are more negatively charged compared to those on lower half (atoms below the central atom “A”). The finer details of the charge distribution (see Figure 3c) show that the positive charge on central atom “A” increases marginally by 0.05 a. u.

The ELF of Al₁₃--N₂ complex is shown in Figure 3a. It is interesting to note that there is lesser polarization of electron density around N₂ as compared to the case of Al₂ and Al₃. This and the fact that the first merging of the basins occurs only at 0.76 isovalue reflects the lower interaction between the Al₁₃ and N₂.

(iv) Structure, Bonding of Al₃₀ and its Interaction with N₂ molecule:

To evaluate the adsorption energy of N₂ molecule as a function of cluster size, we next consider a 30 atom cluster. There have been quite a few recent reports on the lowest energy conformation of Al₃₀. One of the reports has suggested a double tetrahedron as a local minima for Al₃₀.⁵² Recent reports, on the other hand have reported few other conformations as the lowest energy geometry for Al₃₀.^{53, 54} However, we have used the double tetrahedron for the case of N₂ adsorption. The geometries of Al₃₀ and its complex with N₂ and various other properties are given in Figure 4. Based on symmetry, the atoms in the cluster can be classified into 7 types of sites as shown in Figure 4. The inter-atomic distances between various sites are reported in Table 2. It is seen from the Table that the edge atoms are

far from central atom (“E”). These bonds lay in the range 3.78 Å to 6.47 Å. On the other hand, surface atoms F and G lie at optimal distance of 2.75 Å from central atom while their corresponding distances with adjacent surface and edge atoms is slightly longer. The bond lengths among edge atoms viz., “A”-”B” (2.65 Å), “B”-”C” (2.65 Å) and “C”-”D” (2.59 Å) are the shortest ones.

The short bond distance between the edge atoms is well reflected in the ELF plots (see Figure 4). At an isosurface of 0.86 the basins of all edge atoms merge. However, at the same value, the basins on surface atoms remain as such which merge at a lower value of 0.74. The HOMO of this conformation is mainly contributed by “A” and “B” atoms. The LUMO is contributed by “C” and “D”. Considering the FMO contributions, N₂ can preferably adsorb on the edge atoms “A”, “B”, “C”, and “D” atoms.

First, we consider site “A” for N₂ adsorption (see Figure 4). The Al-N and N-N bonds optimize to 1.86 Å and 1.13 Å respectively as in the case of Al₁₃. The interaction energy falls in the same range as observed for the earlier clusters, i. e. 8.01 kcal/mol. The structural details of Al₃₀-N₂ complex are reported in Table 2. Although, the original double tetrahedron is not distorted much, there are some small perturbations following the N₂ adsorption. Notable among them are the inter-atomic distances between site “C” and “D” which increases and consequently, ELF at 0.86 show some disconnected basins. The basin around site A atom, involved in Al-N bond, disappears. The HOMO of the complex is formed of P-P orbital overlap of site C, site D edge and site F, site G surface atoms. However, the LUMO is similar to the LUMO of bare Al₃₀. In addition to this, LUMO is also present on N₂ molecule.

In the above Al₃₀--N₂ complex, the N₂ is adsorbed vertically on the site A. Adsorption of N₂ molecule on sites B and C result in similar interaction energies and electronic properties. We have also attempted a case of multiple bonding where N₂ molecule adsorbs on site B with slight inclination towards site C, forming a bridge. However, this orientation results into a conformation where N₂ adsorbs only on site B atom with more or less same interaction energy.

(v) Structure, Bonding of Al₁₀₀ and its Interaction with N₂ molecule:

We must not forget that the original work reported by Jarrold *et. al.* is on Al₁₀₀ cluster. Hence, to check the N₂ interaction with such a large cluster, we consider one of the potential minima of Al₁₀₀ cluster. It is difficult to illustrate the in detail structural parameters of 100 atom clusters, hence, we only outline the peculiarities found in bonding those obtained from ELF and FMO reported in Figure 5. The Figure 5 shows that most of the Al atoms are clustered on the surface and very few of them form the core. The covalency of Al₁₀₀ cluster is as good as that of symmetrical Al₃₀ cluster. The basins on the surface atoms start merging at an 0.84 isovalue. The HOMO, is centered on many surface atoms, particularly showing the multi-centered bonding resembling that of Ih HOMO. The N₂ is adsorbed on one of the free sites. The interaction energy is 7 kcal/mol with an optimized Al-N bond of 1.91 Å. The N-N elongation, here, is to the same magnitude of 1.13 Å. Similar to small sized Al cluster N₂ complex, ELF does not show and merged basins along Al-N bond. The ELF contours merge at lower isovalue of 0.80 resulting in further reduction of covalency. The HOMO of Al₁₀₀-N₂ is localized on both N atoms and interacting Al atom. On the contrary, N₂ also participates in LUMO formation. Thus, the interaction energy of N₂ molecule with the ground state conformation does not seem to vary substantially with respect to the cluster size.

(b) Structure, Bonding and Interaction of High Energy Al₁₃ conformations with N₂ Molecule:

(i) Decehedron (D_h):

As discussed in Section I, N₂ adsorption on Al clusters increases dramatically above temperatures which correspond to the phase transition of the later. Just below and above the phase transition, clusters visit several high energy conformations. Such high energy conformations exhibit contrastingly different structural and electronic properties (particularly the surface atoms) as compared to the ground state conformations. One of the objectives of this work is to understand if such a change in surface properties can contribute to better adsorption of N₂ (and hence better reactivity) on Al clusters. Hence, we next study some of the high energy conformations of Al clusters and N₂ adsorption on them. For this purpose, we have chosen high energy conformations of Al₁₃ as a case study. It has

been reported earlier that Al_{13} undergoes a phase transition around 1400 K.³⁷ Decahedron is a dominant high energy conformation of Al_{13} seen from 400 K to 1200 K.³⁷ Hence, we found it interesting to study the adsorption of N_2 on this conformation. In addition, we have also chosen two high energy conformations from a finite temperature run of 1600 K. In the next few sections, we discuss the structure and bonding of these high energy conformations and their implications on the N_2 adsorption.

We begin with a discussion on decahedron (D_h). Figure 6 shows the structural details of this conformation. D_h having lower symmetry than that of I_h , the atoms within it can be classified into 5 types. Figure 6 shows five unique sites (as compared to three seen in I_h). The central atom, “A” is bonded to two vertex atoms “B” with an interatomic distance of 2.66 Å. Rest of the ten atoms form two planes between the central atom and two vertex atoms and are classified as “C”, “D” and “E” based on the symmetry (See Figure 6). The inter atomic distances between various sites are tabulated in Table 3. Interestingly, the inter atomic distances between sites “E” and “D” (i. e. “D”-“D” and “E”-“E” bond distances) are 2.59 Å, same as that of Al_2 dimer. Such a short bond distance is indicative of covalent bonding between these atoms. “C”-“C” bonds are the next shortest ones (2.63 Å) Thus, intra-planar atoms are bonded to each other with strong covalent bonds. The inter-planar bond distances viz., “C”-“D” and “D”-“E” are marginally longer with a reasonably large bond distances of 2.70 Å and 2.81 Å, respectively. Rest of the bond distances lay in the order of 2.66-2.72 Å. Analysis of ELF basins reveals the covalent nature of bonding across the two planes. The ELF basins of same sites merge at a high isovalue of 0.90, whereas those across the two planes merge at 0.78 isovalue.(see Figure 6). Thus, D_h conformation is a more covalently bonded conformation as compared to the ground state I_h conformation of Al_{13} . The Mulliken charges on each site are given in Table 3. All the surface atoms are negatively charged resulting in a positively charged central atom. The atoms in the two planes are the most negatively charged ones.

The HOMO and LUMO of D_h are reported in the Figure 6. The HOMO contributed by the

bonding orbitals of p-p overlap between the “C”-“C”, “D”-“D” and “E”-“E” atoms while LUMO is concentrated only on site B i. e. vertex atom. Considering the contribution of various atoms to HOMO and LUMO, we finalize four sites for N₂ interaction, viz., “B”, “C”, “D” and “E”. Interestingly, sites “B” and “C” do not show any reactivity towards N₂ adsorption. All orientations of N₂ on these two sites resulted in high energy structures with N₂ getting finally separated. The presence of highly covalent bonds around site “C” may be a probable reason for desorption on that site, site “B” being least negatively charged may be unfavorable for the N₂ adsorption. However, sites “D” and “E” are better for N₂ adsorption leading to stable complexes. The site E gives elevated interaction energy compared to site D. In both these optimizations although we started with initial D_h geometry, the final complex obtained was nearly I_h--N₂ complex. That is during optimization D_h structure transforms into an I_h structure. This has been found to be the case irrespective of the optimization algorithm and initial orientations of N₂ molecule on these sites. Thus, N₂ adsorbed and stabilized complex is no more D_h--N₂ complex but it is same as original I_h--N₂ complex. This change of geometry reflects in ELF and FMO plots shown in Figure 6 which shows that the contours of this complex are analogous to those in original I_h--N₂ complex. However, the strength of interaction at both sites, D and E, is different. Site E shows almost double interaction energy than that of site D, The interaction energy at site E is 15.86 kcal/mol and the same at site D is 8.28 kcal/mol. These high energies of interaction are obtained from using definition of interaction energy as follows,

$$\text{Interaction Energy} = E_{\text{complex}} - (E_1 + E_2) \quad (1)$$

Where, E_{complex} is energy of complex which is converted to N₂ adsorbed I_h geometry. E_1 is energy of optimized D_h and E_2 is energy of optimized N₂. Since, final complex is no longer D_h, if we substitute E_1 as energy of optimized I_h, both interaction energies (at site D and site E) decrease significantly. In the later case site D is almost not bonded to N₂ (IE ~ 0.0 kcal) where as interaction of site E and N₂ is just same as original I_h--N₂ complex. As a consequence of this D_h turned I_h--N₂ complex shows similar behavior of bonding as described above in I_h section. Rest of the geometrical parameters of this final

complex are same as those found in I_h -- N_2 complex.

(ii) High Energy Conformations H1 and H2:

We next attempt the adsorption of N_2 molecule on some of the high energy Al_{13} conformations which are not so well known. As mentioned earlier, these conformations have been extracted from an molecular dynamical simulation of the Al_{13} -- I_h cluster around 1400 K. Figure 7 gives one of the perspectives of both these two clusters. It is clearly seen that these high energy conformations are distorted leading to as many chemically unequal sites. H1 has nine chemically (Site “A” to Site “I” as shown in Figure 7) unequal sites while H2 has as many sites as the number of atoms within it. The high energy conformation H1 appears to be a hybrid of I_h and D_h conformations. The ELF at an isosurface of 0.90 reveals that both these conformations are characterized by the presence of covalent bonds at few pockets of the clusters. The inter atomic distances between the atoms in the two clusters range from 2.54 to 2.84 Å. The charge distribution as obtained from the Mulliken population analysis for both the conformations is given in Table 4. It is seen from the Table that the atoms on the surface are mostly negatively charged and the central atoms are positively charged. Upon adsorption of N_2 , H1 conformations results in a stable complex with an adsorption energy of 7.65 kcal/mol while adsorption of N_2 on H2 conformations leads to an interaction energy of 13.54 kcal/mol. Interaction energy increases by approximately 5 kcal/mol for a high melted and distorted structure H2, however, the case is not same for H1-- N_2 complex.

Thus, interestingly it appears that varying the cluster size and just the reorientation of the bonds does not contribute significantly to the better adsorption of N_2 on Al clusters. The clear understanding of this elevated strength of interaction in case of H2 conformer can be understood with keen observation of the FMOs. The HOMO (see Figure 7) is dominantly spread over Al (7). In addition this is the least bonded and hence free site. The N_2 is adsorbed in a plane of triangle made up of Al(5), Al(7) and Al(12) atoms. This forms a stable complex with Al-N bond optimized to 1.90 Å. Here, the increase in interaction energy however is not ascribed by nature of H2 directly but is approved by additional Al-

N bond formed between Al(12) and N(1). The characteristic bond formed so is 2.93 Å. The N-N elongation is 1.13 Å. The Al(7)-Al(12) bond in bare H2 is 2.58 Å. In the respective complex, the Al(12) is close to Al(7). This bond reduces to 2.55 Å as N₂ approaches to Al(7) and thus retains a favorable geometry to form another Al-N bond (see Figure 7, H2--N₂ HOMO). There is no specific trend i. e. bond elongation or reduction observed in H2--N₂ complex formation. In general, the bonds in close vicinity of Al(7) show bond reduction. We also summarize the atomic charges on the interacting Al and N atoms. Let us concentrate on the atomic charges which participate in Al-N bond. A positive charge of 0.38 a. u. is built on the Al(7). The Al(12) atom is also bonded with N(1). Hence, the Al(12) pulls charge of -0.34 a. u. from N(1). The N(1) here, hence, acquires slightly less negative charge compared to other N₂ complexes.

Thus after studying various conformers of Al₁₃ and their interaction with N₂, we can conclude that in case of Al₁₃, the N₂ interaction is not just dependent on structural arrangement of atom but is also a function of multiple bonding of N₂ with Al cluster. In other words, the highly melted or deformed structure where adjacent Al-Al bonds are not so strongly coordinated, N₂ can interact to form various Al-N bonds resulting in highly stable (Al)_n--N₂ complex. This is validated by the analysis of average interatomic Al-Al distances in Al₁₃ clusters. The average interatomic distance shows a substantial increase in H2, a highly melted structure (3.91) as compared to 3.59, 3.65 and 3.70 in Ih, Dh and H1 respectively. Here, we must address that N₂ adsorption is carried out on a melted structure obtained after phase transition and no temperature effect is considered while its interaction. Thus, to count its chemisorption as mentioned by Jarrold *et. al.* we must bring in the thermal effects with the help of dynamics. Hence, in our next paper, we plan to study the high temperature thermodynamics to obtain highly melted 100 atom cluster, followed by the room temperature reaction of N₂ adsorption.

IV. Conclusion and Scope

Density Functional Calculations have been carried out to understand the adsorption of the N₂ molecule on the ground state geometries of Al_n clusters (n=2, 3, 13, 30, 100). The studies were also

extended to few high energy conformations of Al_{13} . We summarize the adsorption energies of N_2 molecule on these ground state geometries and high energy conformations of Al_{13} clusters in Figure 8. With the exception of Al_2 , all other ground state conformations show interaction energy between 8-10 kcal/mol. As seen from the figure, the interaction energy is stable with respect to the cluster size. This interaction is mostly accompanied by a charge transfer from Al atoms to the nitrogen atoms in the complex. The bonding within ground state geometries in all cluster sizes is partially covalent and partially metallic. However, the extent of covalency is seen to vary to some extent between the various sized clusters. Thus, independent of the electronic and structural properties, N_2 interacts weakly (an ionic bond) with the ground state geometries of Al clusters. The presence of high energy conformations of Al_{13} on the N_2 adsorption is seen to give mixed results with some high energy conformations leading to similar interaction energies as that of a ground state conformation (Decahedron and H1), whereas, high energy conformation of Al_{13} , viz., H2 is seen to favor the N_2 adsorption better due to the presence of more than one Al-N bond. Such multiple bonds between the ligand molecule and cluster are, thus, a characteristic phenomenon of high temperatures. This is a consequence of increased interatomic distances between the Al-Al atoms (and thus weaker bonds) following the melting. Thus, the above work indicates that the enhancement of reactivity of melted Al clusters is more due to thermodynamic factors and electronic factors play a minor role in the increasing adsorption energy of N_2 molecule.

Acknowledgments

One of the authors (BSK) acknowledges CSIR (Council of Scientific and Industrial Research) for funding of the SRF (Senior Research Fellowship). We acknowledge the Center of Excellence in Scientific Computing at NCL. SP acknowledges the J. C. Bose Fellowship grant of DST towards partial fulfillment of this work.

References:

- ¹ B. Cao, A. K. Starace, O. H. Judd, M. F. Jarrold, *J. Am. Chem. Soc.* **131**, 2446 (2009).
- ² R. Ferrando, J. Jellinek, R. L. Johnston, *Chem. Rev. Washington, D. C.* **108**, 845, (2008).
- ³ A. O. Orlov, I. Amlani, G. H. Bernstein, C. S. Lent, G. L. Snider, *Science* **277**, 928 (1997).
- ⁴ M. Valden, X. Lai, D. W. Goodman, *Science* **281**, 1647 (1998) .
- ⁵ A. A. Shvartsburg, M. F. Jarrold, *Phys. Rev. A* **60**, 1235 (1999).
- ⁶ A. Aguado and J. M. Lopez, *J. Chem. Phys.* **130**, 064704 (2009).
- ⁷ A. Lechtken, C. Neiss, M. M. Kappes, D. Schooss, *Phys. Chem. Chem. Phys.* **11**, 4344 (2009).
- ⁸ E. C. Honea, A. Ogura, D. R. Peale, C. Felix, C. A. Murray, K. Raghavachari, W. O. Sprenger, M. F. Jarrold, W. L. Brown, *J. Chem. Phys.* **110**, 12161 (1999).
- ⁹ C. Bracchignac, P. Cahuzac, J. Leygnier, J. Weiner, *J. Chem. Phys.* **90**, 1492 (1989).
- ¹⁰ U. Ray, M. F. Jarrold, J. E. Bower, J. S. Kraus, *J. Chem. Phys.* **91**, 2912 (1989).
- ¹¹ D. A. Hales, L. Lian, and P. B. Armentrout, *Int. J. Mass Spectrom. Ion Process.* **102**, 269 (1990).
- ¹² M. Schmidt, R. Kusche, B. von Issendorf, and H. Haberland, *Nature (London)* **393**, 238 (1998).
- ¹³ C. M. Neal, A. K. Starace, and M. F. Jarrold, *Phys. Rev. B* **76**, 054113 (2007).
- ¹⁴ C. Hock, C. Bartels, S. Strayburg, M. Schmidt, H. Haberland, B. von Issendorff, and A. Aguado, *Phys. Rev. Lett.* **102**, 043401 (2009).
- ¹⁵ S. M. Ghazi, S. Zorriasatein, and D. G. Kanhere, *J. Phys. Chem. A* **113**, 2659 (2009).
- ¹⁶ G. A. Breaux, B. Cao, and M. F. Jarrold, *J. Phys. Chem. B* **109**, 16575 (2005).
- ¹⁷ C. M. Neal, A. K. Starace, M. F. Jarrold, K. Joshi, S. Krishnamurty, and D. G. Kanhere, *J. Phys. Chem. C* **111**, 17788 (2007).
- ¹⁸ E. G. Noya, J. P. K. Doye, D. J. Wales, and A. Aguado, *Eur. Phys. J. D* **43**, 57 (2007).
- ¹⁹ K. Joshi, S. Krishnamurty, and D. G. Kanhere, *Phys. Rev. Lett.* **96**, 135703 (2006).
- ²⁰ K. Manninen, A. Rytnen, and M. Manninen, *Eur. Phys. J. D* **29**, 39 (2004).
- ²¹ S. Chacko, K. Joshi, and D. G. Kanhere, *Phys. Rev. Lett.* **92**, 135506 (2004).

- ²² (a) G. A. Breaux, C. M. Neal, B. Cao, M. F. Jarrold, *Phys. Lett.* **94**, 173401 (2005). (b) C. M. Neal, A. K. Starace, M. F. Jarrold, *J. Am. Soc. Mass Spectrum.* **18**, 74 (2007).
- ²³ (a) M. Costantino, C. Fipro, *J. Mater. Res.* **6**, 2397 (1977). (b) V. V. Zakorzhevskii, I. P. Borovinskaya, N. V. Sachkova, *Inorg.* **38**, 1131 (2002).
- ²⁴ O. Mayer, E. Z. Fromm, *Mettallkunde* **68**, 27 (1977).
- ²⁵ Z. Romanowski, S. Krukowski, I. Grzegory, S. Porowski, *J. Chem. Phys.* **114**, 6353 (2001).
- ²⁶ G. Kresse, J. Hafner, *J. Phys. Rev. B* **48**, 13115 (1993).
- ²⁷ G. Kresse, J. Furthermuller, *Comput. Mater. Sci.* **6**, 15 (1996).
- ²⁸ W. Kohn and L. J. Sham, *Phys. Rev.* **140**, 1133 (1965).
- ²⁹ D. Vanderbilt, *Phys. Rev. B* **41**, 7892 (1990).
- ³⁰ J. P. Perdew, Y. Wang, *Phys. Rev. B* **45**, 13244, (1992).
- ³¹ M. C. Payne, M. P. Teter, D. C. Allan, T. A. Arias, J. D. Joannopoulos. *Rev. Mod. Phys.* **64**, 1045 (1992).
- ³² P. Pulay, *Chem. Phys. Lett.* **73**, 393, (1980).
- ³³ B. Silvi, A. Savin, *Nature (London)* **371**, 683, (1994).
- ³⁴ R. G. Parr and W. Yang, *J. Am. Chem. Soc.* **106**, 4049 (1984).
- ³⁵ Y. Yang and R. G. Parr, *Proc. Natl. Acad. Sci. USA* **821**, 6723 (1985).
- ³⁶ (a) W. Yang and W. Mortier, *J. Am. Chem. Soc.* **108**, 5708 (1986). (b) M. W. Schmidt, K. K. Baldrige, J. A. Boatz, S. T. Elbert, M. S. Gordon, J. H. Jensen, S. Koseki, N. Matsunga, K. A. Nguyen, S. Su, T. L. Windus, M. Dupuis and J. A. Montgomery *J. Comput. Chem.* **14**, 1347 (1993).
- ³⁷ P. Chandrachud, K. Joshi. D. G. Kanhere, *Phys. Rev. B*, **76**, 235423 (2007).
- ³⁸ S. Nóse, *Mol. Phys.* **52**, 255 (1984).
- ³⁹ A. Bogicevic, P. Hyldgaard, G. Wahnstrom, B. I. Lundqvist, *Phys. Rev. Lett.* **81**, 172 (1998).
- ⁴⁰ J. Akola, H. Hakkinen, M. Manninen, *Phys. Rev. B* **58**, 3601 (1998).

- ⁴¹ A. I. Boldyrev, P. v. R. Schleyer, *J. Am. Chem. Soc.* **113**, 9045 (1991).
- ⁴² R. O. Jones, *J. Chem. Phys.* **99**, 1194 (1993).
- ⁴³ B. K. Rao, P. Jena, *J. Chem. Phys.* **111**, 1890 (1999).
- ⁴⁴ Z.J. Li, J.H. Li, *Solid state communications*, **149**, 375 (2009).
- ⁴⁵ J. Moc, *The European Physical Journal, D*, **45**, 247 (2007).
- ⁴⁶ C. H. Yao, S. F. Zhao, J. R. Li, Y. W. Mu, J. G. Wan, M. Han and G. H. Wang, *Eur. Phys. J. D.*, **57**, 197 (2010).
- ⁴⁷ A. C. Reber, S. N. Khanna, P. J. Roach. W. H. Woodward and A. W. Castleman. Jr. *J. Am. Chem. Soc.* **129**, 16098 (2007).
- ⁴⁸ R. O. Jones, *Phys. Rev. Lett.* **67**, 224 (1991).
- ⁴⁹ H. Basch, *Chem. Phys. Lett.* **136**, 289 (1987).
- ⁵⁰ U. Rothlisberger, W. Andreoni, P. Giannozzi, *J. Chem. Phys.* **96**, 1248 (1992).
- ⁵¹ *Theory of Orientation and Stereo Selection* by K. Fukui (Springer-Verlag, Berlin 1975).
- ⁵² W. Zhang, W-C. Lu, J. Sun, C. Z. Wang, K. M. Ho, *Chem. Phys. Lett.* **455**, 232 (2008).
- ⁵³ N. Drebov, R. Alrichs, *J. Chem. Phys.* **132**, 164703 (2010).
- ⁵⁴ A. Aguado, J. M. Lopez, *J. Chem. Phys.* **130**, 064704, (2009).

Table 1: Structural and Electronic Properties of Al₁₃ (I_h) and its N₂ Complex

Distance (Å)	I_h	I_h--N₂
A-C _{int}	-	2.63
A-B	2.66	2.65
A-C	2.60	2.54
Al-N	-	1.90
N-N	1.11	1.13
B-C	2.70	2.78
B-B (diagonally placed)	5.32	5.50
B-B	2.82	2.85
C-C (diagonally placed)	5.21	5.28
C-C	2.90	2.86
Interaction energy (kcal/mol)	-	7.91
Average Charges on various sites as obtained from Mulliken population analysis (a. u.)		
Sites	I_h	I_h--N₂
A	3.43	3.49
B	-0.3	-0.51, -0.52, -0.49, -0.30, -0.30, -0.27
C _{int}	-0.3	0.81
C	-0.28	-0.49, -0.36, -0.41, -0.28, -0.26
N(1)	-	-0.22
N(2)	-	0.1

Table 2: Structural and Electronic Properties of Al₃₀ and its N₂ Complex

Distance (Å)	Al₃₀	Al₃₀--N₂
A-B	2.66	2.54
A-E	6.47	6.00
B-B	2.86	2.91
B-C	2.65	2.58
B-F	2.76	2.69
B-E	4.69	4.60
C-C	2.68	2.70
C-F	2.68	2.74
C-D	2.59	2.63
C-G	2.74	2.64
F-G	2.64	2.62
C-E	3.78	3.90
F-E	2.75	2.84
D-G	2.65	2.68
G-G	2.52	2.65
G-E	2.75	2.80
D-E	4.51	4.77
Al-N	-	1.86
N-N	1.11	1.13
Interaction energy (kcal/mol)	-	8.01

Table 3: Structural and Electronic Properties of Al₁₃ (D_h) and its N₂ Complex

Distance (Å)	D_h	D_h--N₂ (I_h--N₂)
A-B	2.66	2.66
A-C	2.66	2.62
A-D	2.69	2.66
A-E	2.69	2.53
Al-N	-	1.90
N-N	1.11	1.13
B-C	2.69	2.79
B-D	2.72	2.73
B-E	2.67	2.70
B-B	5.32	5.28
C-D	2.70	2.78
C-E	4.42	4.31
C-C	2.63	2.78
D-E	2.81	2.68
D-D	2.59	2.77
E-E	2.59	2.74
Interaction energy (kcal/mol)	-	15.86
Average Charges on various sites as obtained from Mulliken population analysis (a. u.)		
Sites	D_h	D_h--N₂ (I_h--N₂)
A	2.93	3.49
B	-0.10	-0.31, -0.51
C	-0.30	-0.26, -0.35, -0.30, -0.30
D	-0.26	-0.50, -0.34
E	-0.24	0.77, -0.40
N(1)	-	-0.21
N(2)	-	0.10

Table 4: Electronic Properties of H1, H2 (Al₁₃) and its N₂ Complex

Sites	H1	H1--N ₂
Average Charges on various sites as obtained from Mulliken population analysis (a. u.)		
A	2.07	1.61
B	-0.16	1.46
C	-0.01	-0.18
D	-0.20	-0.25
E	-0.36	-0.26
F	-0.28	0.00
G	-0.37	-0.43
H	-0.07	-0.25
I	0.01	0.00
N(1)	-	-0.22
N(2)	-	0.09
Interaction energy (kcal/mol)	-	7.65

Sites	H2	H2--N ₂
Average Charges on various sites as obtained from Mulliken population analysis (a. u.)		
1	1.22	1.20
2	-0.17	-0.38
3	0.11	0.22
4	-0.53	-0.46
5	0.34	0.17
6	-0.14	-0.34
7	-0.49	0.38
8	-0.13	-0.19
9	-0.54	-0.42
10	0.17	-0.02
11	0.42	0.44
12	-0.26	-0.34
N(1)	-	-0.18
N(2)	-	0.09
Interaction energy (kcal/mol)	-	13.54

Figure 1: Al₂ and its N₂ interaction from ELF and FMO

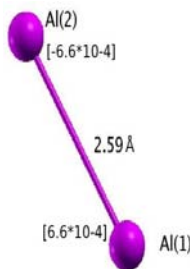
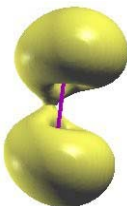
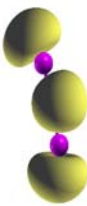
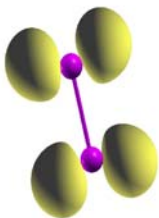
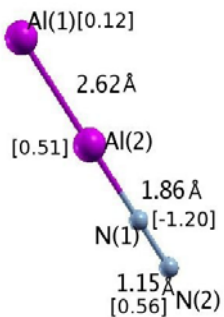


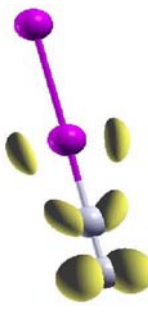
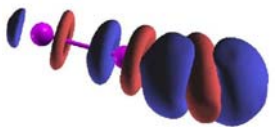
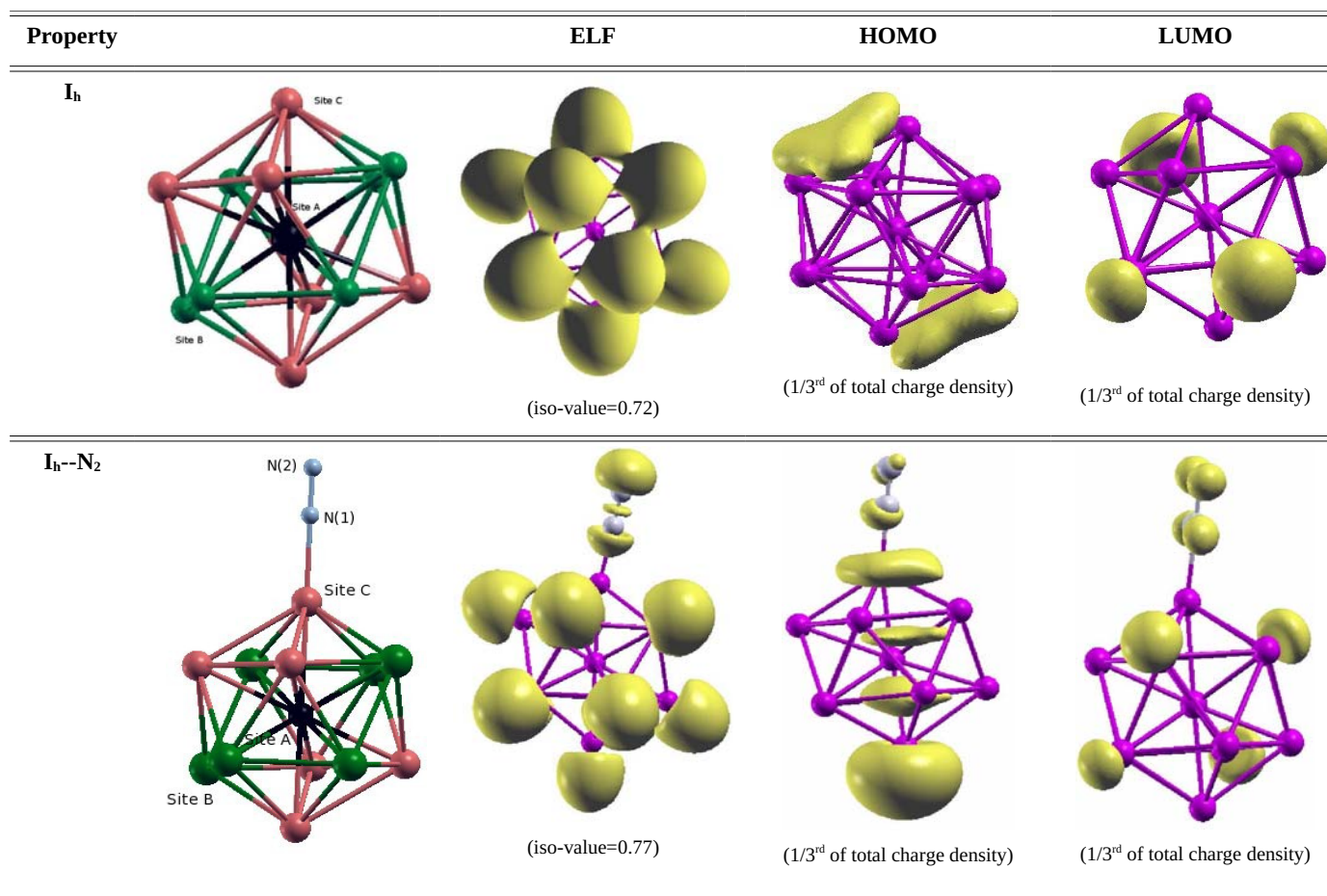
Property		ELF	HOMO	LUMO
Al ₂	 <p>Al(2) [-6.6*10-4] 2.59 Å [6.6*10-4] Al(1)</p>	 <p>(iso-value=0.78)</p>	 <p>(1/3rd of total charge density)</p>	 <p>(1/3rd of total charge density)</p>
Al ₂ --N ₂	 <p>Al(1)[0.12] 2.62 Å [0.51] Al(2) 1.86 Å N(1) [-1.20] 1.15 Å [0.56] N(2)</p>	 <p>(iso-value=0.76)</p>	 <p>(1/3rd of total charge density)</p>	 <p>(1/3rd of total charge density)</p>
Difference Charge Density				

Figure 2: Al₃ and its N₂ interaction from ELF and FMO

Property	ELF	HOMO	LUMO	
Al ₃		<p>(iso-value=0.74)</p>	<p>(1/3rd of total charge density)</p>	<p>(1/3rd of total charge density)</p>
Al ₃ --N ₂		<p>(iso-value=0.80)</p>	<p>(1/3rd of total charge density)</p>	<p>(1/3rd of total charge density)</p>
Difference Charge Density				

Figure 3a: Al_{13} (I_h) and its N_2 interaction from ELF and FMO



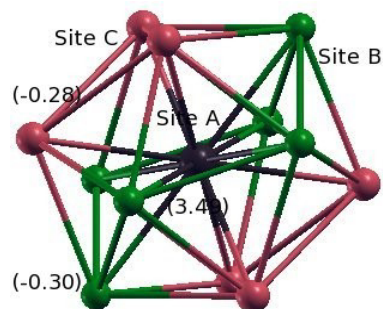


Figure 3b: $Al_{13}(I_h)$ another perspective.

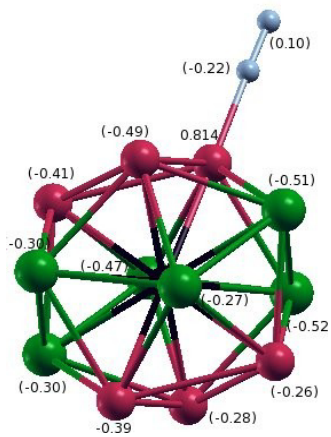


Figure 3c: $Al_{13}(I_h--N_2)$ another perspective.

Figure 4: Al_{30} and its N_2 interaction from ELF and FMO

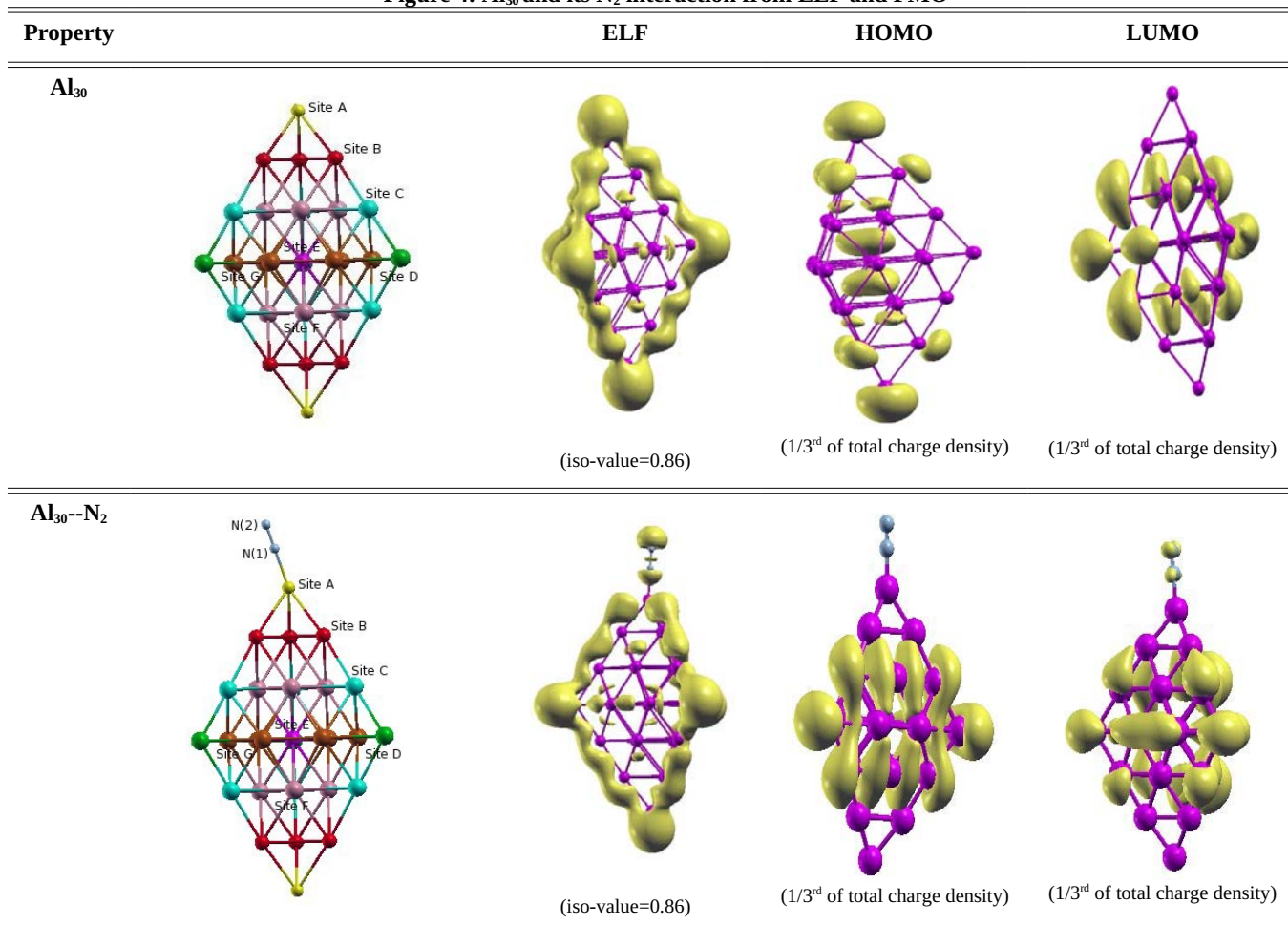


Figure 5: Al_{100} and its N_2 interaction from ELF and FMO

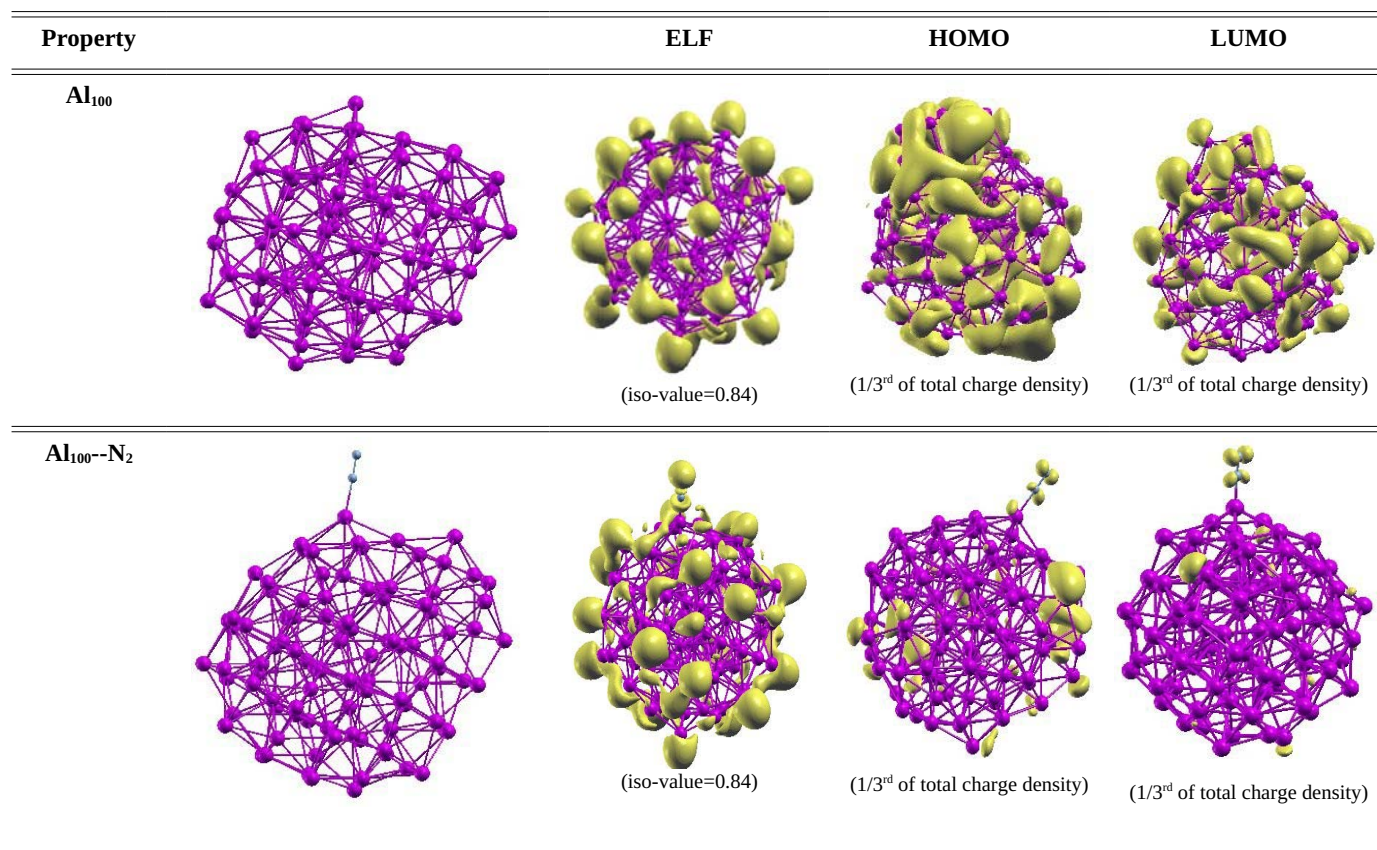


Figure 6: Al_{13} (D_h) and its N_2 interaction from ELF and FMO

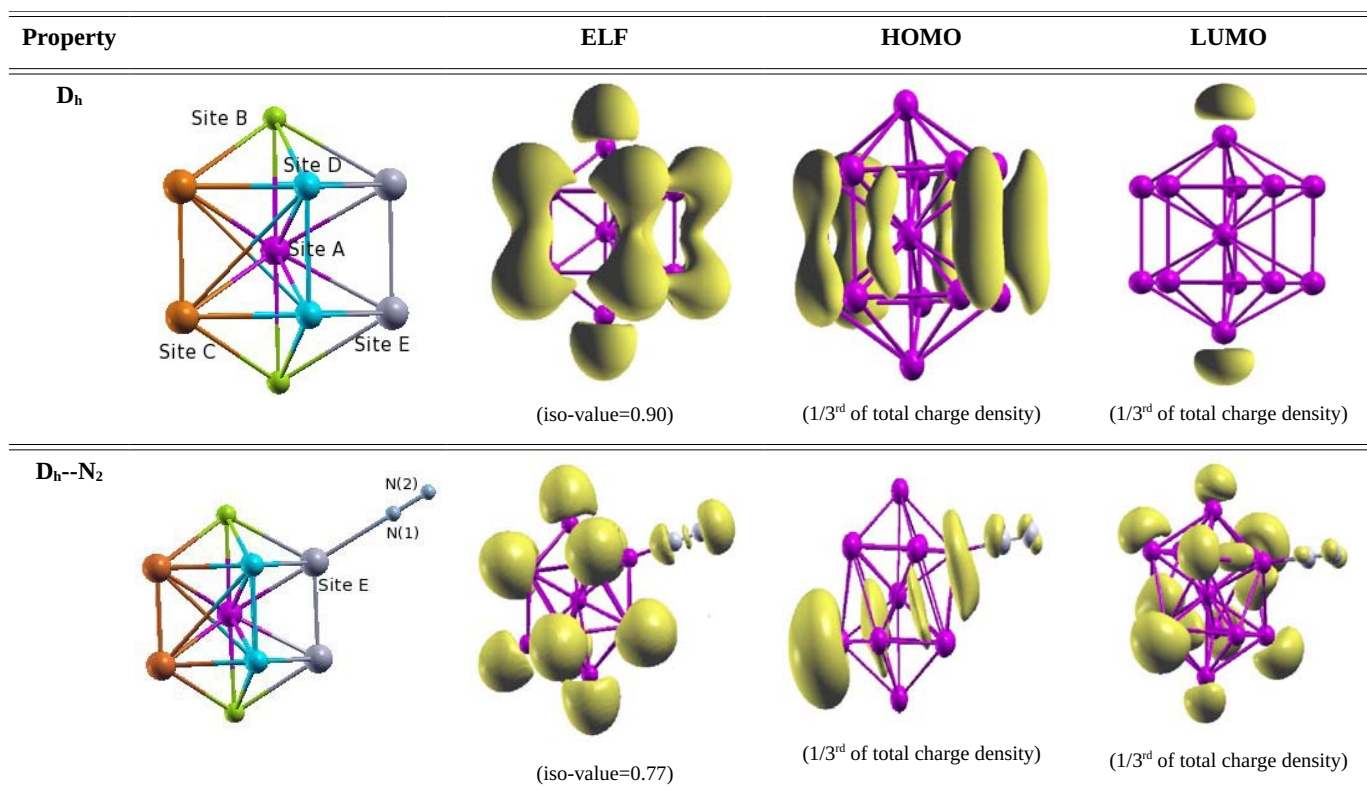
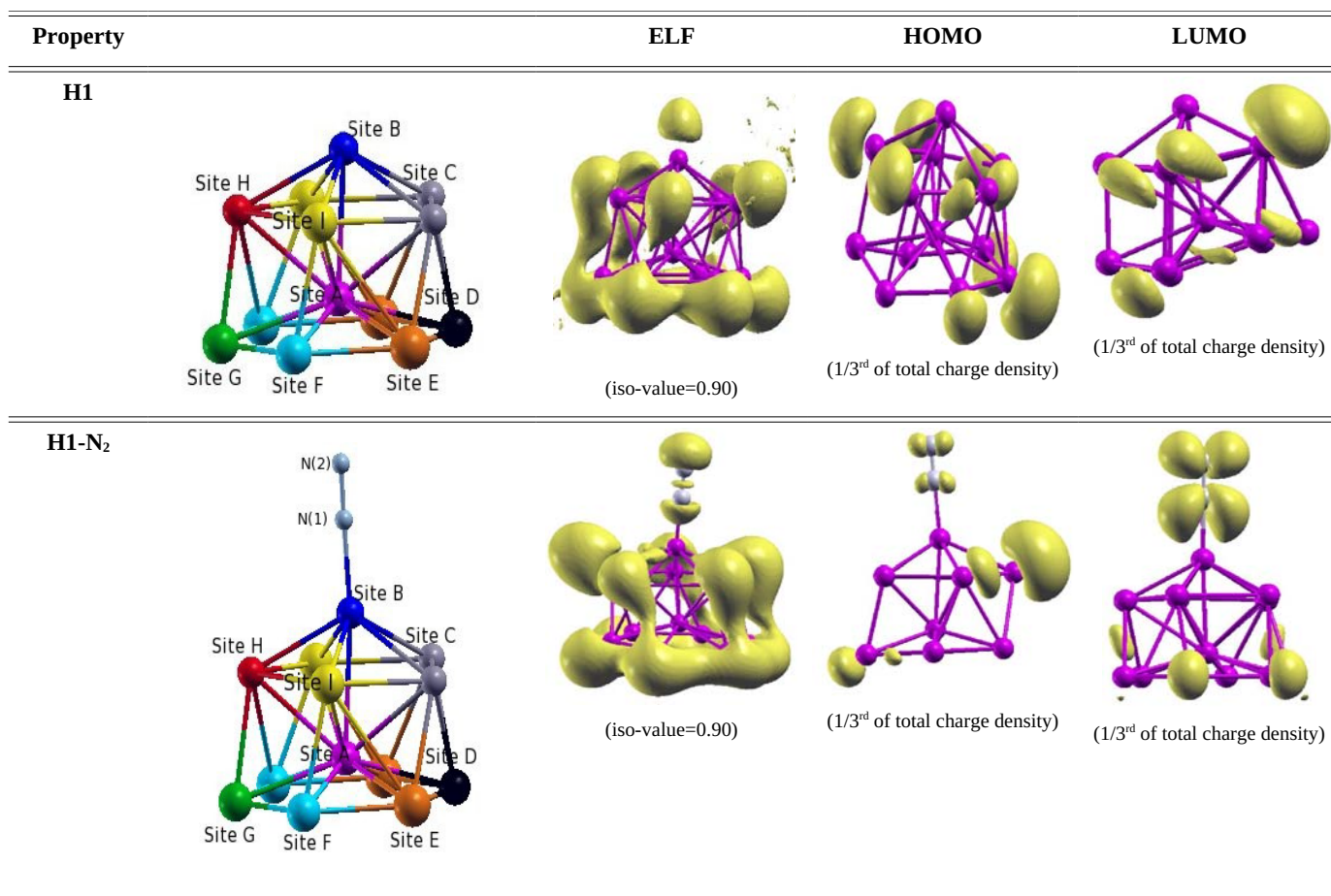
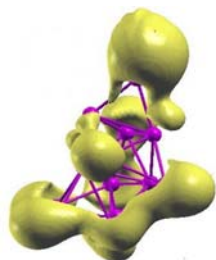
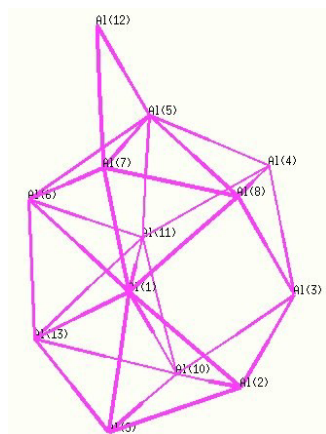


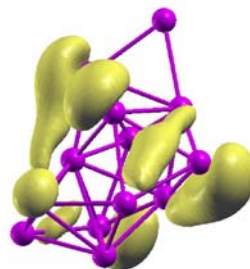
Figure 7: Al₁₃ high energy configurations and its N₂ interaction from ELF and FMO



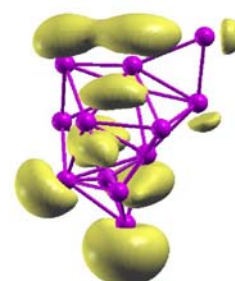
H2



(iso-value=0.90)

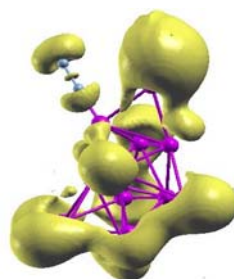
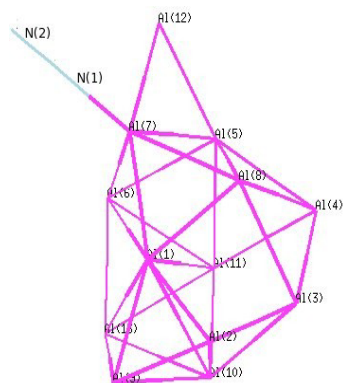


(1/3rd of total charge density)

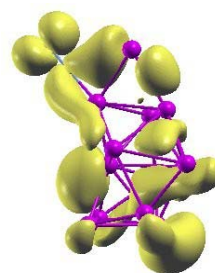


(1/3rd of total charge density)

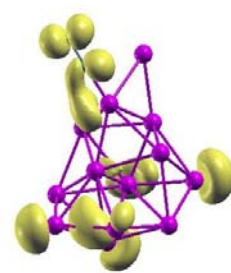
H2--N₂



(iso-value=0.90)



(1/3rd of total charge density)



(1/3rd of total charge density)

Figure 8: Interaction energy as a function of cluster size

